J. Fluid Mech. (1996), vol. 326, pp. 239–263

Dynamics of drop formation from a capillary in the presence of an electric field

By XIAOGUANG ZHANG[1] AND OSMAN A. BASARAN[2]†

[1] Chemical Technology Division, Oak Ridge National Laboratory, Oak Ridge, TN 37831-6224, USA

[2] School of Chemical Engineering, Purdue University, W. Lafayette, IN 47907-1283, USA

(Received 16 August 1995 and in revised form 25 May 1996)

This paper reports an experimental study of the effects of an externally applied electric field on the dynamics of drop formation in the dripping mode from a vertical metal capillary. The fluid issuing out of the capillary is a viscous liquid, the surrounding ambient fluid is air, and the electric field is generated by establishing a potential difference between the capillary and a horizontal, circular electrode of large radius placed downstream of the capillary outlet. By means of an ultra-high-speed video system that is capable of recording up to 12000 frames per second, special attention is paid to the dynamics of the liquid thread that connects the primary drop that is about to detach and fall from the capillary to the rest of the conical liquid mass that is hanging from it. The experiments show that as the strength of the electric field increases, the volume of the primary drop decreases whereas the maximum length attained by the thread increases. The reduction in the volume of primary drops and the increase in the length of threads occur because the effective electromechanical surface tension of the fluid interface falls as the field strength rises. For the highly conducting drops of aqueous NaCl solutions studied in this work, the increase in thread length is due solely to the rising importance of normal electric stress relative to the falling importance of surface tension. However, as the conductivity of the drop liquid decreases, the thread length is further increased on account of the stabilizing influence exerted by the increasing electric shear stress that acts on the charged liquid–gas interface. Two new phenomena are also reported that have profound implications for electrohydrodynamics and practical applications. First, it is shown that whereas the liquid thread always ruptures at its downstream end in the absence of an applied electric field or when the field strength is low, it ruptures at its upstream end when the field strength is sufficiently high. Since satellite drops are produced directly from the thread once both of its ends have ruptured, the change in the mechanism of breakup with field strength influences the dynamics and fate of satellite drops. Second, it is demonstrated that the generation of satellites, which are often undesirable in applications, can be suppressed by the judicious application of an electric field. This is accomplished by using a field of moderate strength to induce charges of the opposite sign on the nearby surfaces of the satellite drop and the liquid that remains pendant from the tube following thread rupture. At high field strengths, induced charge effects are too weak to compete with net charge effects: the satellite is repelled by the pendant drop and falls under gravity as a distinct entity.

---

† Present address: School of Chemical Engineering, Purdue University, W. Lafayette, IN 47907-1283, USA.

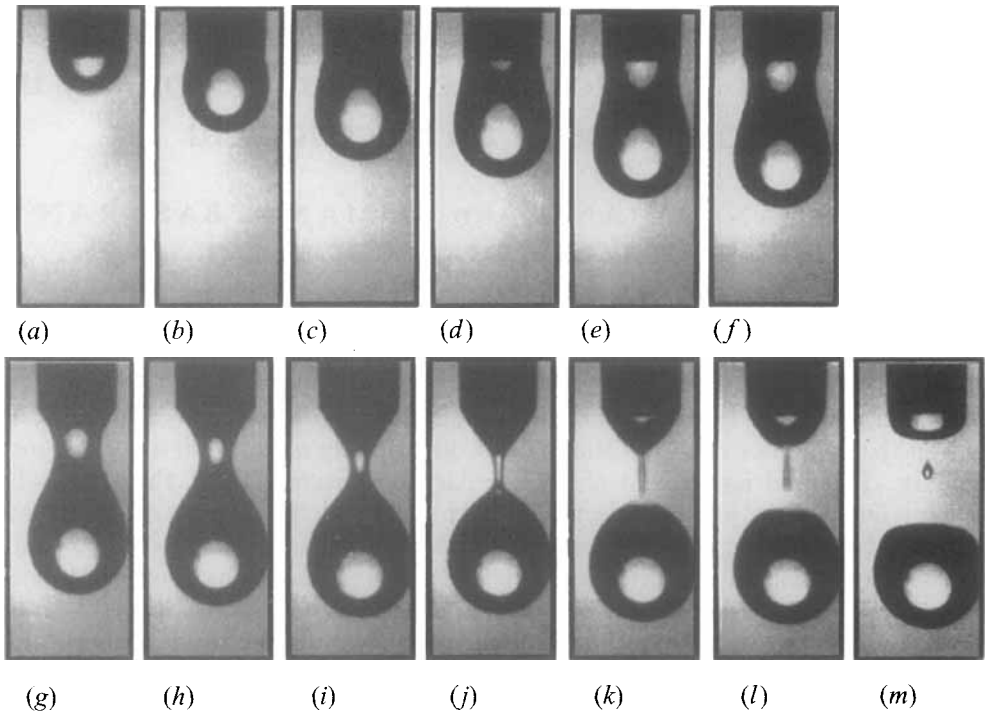

FIGURE 1. Evolution in time t of the shape of a water drop forming out of a capillary of outer radius of 0.16 cm at the liquid flow rate of 1 ml min^{-1} in the absence of an electric field, where t is the time measured from the instant when the previous drop detaches. (*a*) $t = 50$ ms, (*b*) $t = 1090$ ms, (*c*) $t = 2092$ ms, (*d*) $t = 2590$ ms, (*e*) $t = 2990$ ms, (*f*) $t = 3040$ ms, (*g*) $t = 3075$ ms, (*h*) $t = 3083$ ms, (*i*) $t = 3087$ ms, (*j*) $t = 3089$ ms, (*k*) $t = 3090$ ms, (*l*) $t = 3090.5$ ms, and (*m*) $t = 3093$ ms.

1. Introduction

The imposition of an external electric field during the formation of liquid drops from a nozzle or an orifice plate either has been proposed as a technique having great potential or already is employed in a number of technologies. Indeed, electric fields find use in applications as diverse as (i) enhancing rates of mass and/or heat transfer in solvent extraction operations by creating large amounts of interfacial surface area and intense fluid circulation within and around drops (Wham & Byers 1987) and (ii) controlling the volume and orientation of drops in electropainting (Inkpen & Melcher 1987) and ink-jet printing (Fillmore, Buehner & West 1977) by assisting the breakup and deflection of charged drops. The basic unifying feature behind these diverse applications is the electrical force which is due to the applied electric field: the electrical force acts on the fluid–fluid interface and disrupts it to produce a number of charged drops. The aforementioned applications have demonstrated the importance of understanding the dynamics of drop formation in designing and controlling these processes to obtain certain desired characteristics of the drops. In this paper, an experimental study is presented of the dynamics of drop formation in the regime prior to electrospraying where drops of uniform sizes are formed at a constant frequency in time into ambient air directly from the tip of a vertical metal capillary tube that is maintained at a high electrical potential relative to a horizontal grounded electrode placed a distance downstream of the tube outlet. This regime is characterized by both electric fields of moderate strengths and low liquid flow rates.

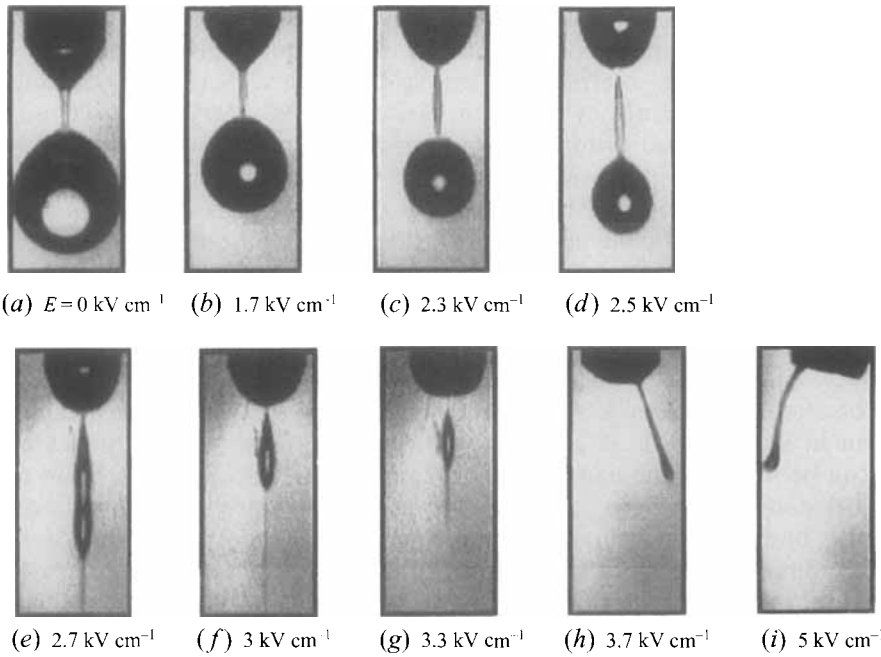

FIGURE 2. The effect of an electric field on the formation of a water drop from a capillary of outer radius of 0.16 cm at the liquid flow rate of 1 ml min^{-1}.

In the absence of an electric field, as a liquid continuously flows at low flow rates through a capillary whose tip opens into another quiescent, immiscible fluid, the liquid being ejected emanates from the capillary as discrete drops under its own weight. This mode of drop formation is often referred to as the dripping mode (e.g. Zhang & Basaran 1995) and is depicted in figure 1. When subjected to an electric field of low strength, the liquid continues to drip from the capillary periodically in time as a series of uniformly sized drops, as shown in figure 2(*a–d*). In the presence of an external electric field, conductive species that are present within a drop migrate to the drop surface, creating a distribution of net electric charge on the interface. This charge distribution then interacts with the external electric field to produce an electric force on the drop. It is well known in the literature that the application of an electric field lowers the effective electromechanical surface tension of the drop–ambient fluid interface (Miller & Scriven 1970; see also Rayleigh 1882 and Basaran & Scriven 1990). Figure 2(*a–d*) shows that there are two gross consequences of the lowering of the effective electromechanical tension in drop formation at low flow rates and low values of the field strength. First, the electric force supplements the gravitational force to elongate the drop. Second, it reduces the size of primary drops that break off the capillary. As the field strength increases, the dripping rate, or the dripping frequency, increases and, correspondingly, the size of drops being formed decreases continuously. When the field strength exceeds a critical value, the mode of drop emission changes from dripping to electrohydrodynamic (EHD) jetting, as shown in figure 2(*e–i*) (Bailey 1988; Cloupeau & Prunet-Foch 1990).

Because of its potential in producing drops that are several orders of magnitude smaller in size than the capillary radius, the formation of charged drops in an electric field has been studied in great detail by numerous investigators for nearly a century since Zeleny's (1915, 1917) pioneering works on the subject. These studies have been

primarily of two types. The first type has attracted most of the attention to date and has focused on computational analysis of the equilibrium shapes and stability of pendant drops in an electric field (see e.g. Basaran & Scriven 1982; Joffre *et al.* 1982), as reviewed recently by Harris & Basaran (1993, 1995). The second type of investigation has focused primarily on experimental studies of atomization by EHD jetting (see e.g. Hayati, Bailey & Tadros 1986; Cloupeau & Prunet-Foch 1990). Upon transition from dripping to EHD jetting, drop emission takes place as a long and narrow but axisymmetric filament, or a jet, that is ejected from the tip of the pendant drop, as shown in figure 2(*e–g*), and breaks into a series of small droplets. As the field strength continues to increase above the value at which transition from dripping to EHD jetting occurs, a point is reached beyond which the emission of droplets from the surface of the pendant drop is no longer axisymmetric: the droplets are created by the breakup of annular jets that are emitted from the rim of the pendant drop, as shown in figure 2(*h–i*). A comprehensive review of the various modes of EHD jetting can be found in the paper by Cloupeau & Prunet-Foch (1990). More recently, theoretical studies have been carried out which report order of magnitude estimates of the sizes of drops and the current emitted during EHD jetting in an axisymmetric mode of atomization referred to as the cone-jet mode (e.g. Fernandez de la Mora & Loscertales 1994). However, the complex free boundary and three-dimensional nature of the general electroatomization problem have so far precluded the development of a complete theoretical understanding.

By contrast, there have been few studies of the effects of an electric field on drop formation from a nozzle via the dripping mode at low flow rates. Moreover, most of the previous theoretical as well as experimental works have been aimed at predicting certain gross features of the dynamics, namely the sizes of and the amounts of surface charge carried by the drops as they break off the nozzle as functions of the strength and orientation of the electric field, fluid properties, and nozzle types (Takamatsu *et al.* 1981; Takamatsu, Yamaguchi & Katayama 1983; Vu & Carleson 1986; Byers & Perona 1988). Unfortunately, the theoretical analyses presented in all of these papers have been based on macroscopic balances in which approximate expressions are used for electrostatic, gravitational, and capillary forces on the drops and inertial forces are neglected. Notwithstanding the approximations made in them and despite the slightly different approaches that they adopt in determining electrostatic forces, the predictions of these previous works exhibit surprisingly satisfactory agreement with the experimental measurements over certain ranges of the parameter space.

Although the previously cited studies of drop formation in the electrostatic dripping mode have captured some of the gross features of the phenomenon, they have done little to elucidate the effects of an electric field on the dynamics of the process, namely the evolution in time of the shape of the forming drop and the catastrophic rupture of the interface of the growing drop to form discrete drops. By contrast, in the absence of an electric field, a number of recent theoretical and experimental studies have greatly improved our understanding of the dynamics of a growing drop by focusing in particular on the evolution in time of the drop profile for times preceding, at, and following the instant of drop detachment from a capillary (Peregrine, Sholer & Symon 1990; Shi, Brenner & Nagel 1994; Eggers & Dupont 1994; Schulkes 1994; Zhang & Basaran 1995). As shown in these studies and summarized in figure 1 with the aid of a time sequence of shapes of a water drop forming from a circular cylindrical capillary into ambient air (cf. Zhang & Basaran 1995), initially the drop gradually elongates from nearly spherical to pear-shaped as its volume increases (figure 1*a–f*). As time advances, the throat of the pear-shaped drop takes on the appearance of a

liquid thread that connects the bottom portion of the drop that is about to detach to the rest of the liquid that is pendant from the capillary (figure 1*g–j*). Thereafter, the thread extends rapidly and breaks up, resulting in the creation of a primary drop and a satellite droplet (figure 1*j–m*). In their experimental study, Zhang & Basaran (1995) have probed quantitatively the effects of physical and geometric parameters on the universal features of drop formation, in particular the development, extension, and breakup of the liquid thread and the generation of satellite droplets subsequent to thread breakup. A detailed understanding of drop formation in the presence of an electric field at the level of Zhang & Basaran (1995) is lacking. Providing this missing understanding is the major goal of this paper.

An experimental program of research is described in this paper that is based on growing a drop at a constant flow rate at the tip of a vertical capillary in the presence of an electric field and monitoring the entire transient evolution of the drop shape on a time scale down to $\frac{1}{12}$ ms. Section 2 summarizes the key parameters that completely govern the electrohydrodynamics of drop formation and identifies certain measures used to characterize drop elongation in subsequent parts of the paper. Section 3 describes briefly the experimental apparatus and methods of data acquisition and analysis. Section 4 details the experimental results and findings. Concluding remarks are the subject of §5.

2. Physics of drop formation in an electric field

In the experiments carried out in this work, a drop of an incompressible Newtonian liquid of constant density ρ and constant viscosity μ is grown at a constant flow rate Q into a quiescent, ambient fluid – here air – from the tip of a vertical, circular cylindrical metal capillary, as shown in figure 3. The ambient fluid exerts uniform pressure and negligible viscous drag on the growing drop. The interface separating the drop liquid and the ambient fluid has surface tension σ. The capillary tube has inner and outer radii, R_i and R, respectively. The drop liquid preferentially wets the metal capillary compared to the ambient fluid so that the three-phase contact line is pinned to the outer sharp edge of the tube. The electric field is created by maintaining the metal capillary at a high electrical potential U_0 relative to a horizontal, circular grounded metal plate that is placed a vertical distance H from the tip of the capillary. The length of the capillary and the radius of the grounded plate both are much larger than the outer radius of the capillary R. The drop and ambient fluids are linearly polarizable and have constant permittivities ϵ and ϵ_o, respectively. The drop liquid is neither a perfect conductor nor a perfect insulator (see §3 and §4); liquid conductivity is constant and denoted by γ.

The dynamics of drop formation in the presence of an electric field is governed by the following dimensionless groups: Re, G, Ca, N_e, K, Pe, R_i/R, and H/R. The non-dimensionalization is carried out here by using R as the length scale, the flow rate divided by the cross-sectional area based on the outer radius of the capillary, $u \equiv Q/\pi R^2$, as the velocity scale, σ/R as the pressure scale, and U_0 as the electrostatic potential scale. $Re \equiv \rho u R/\mu$ is the Reynolds number that measures the relative importance of inertial and viscous forces. $G \equiv \rho R^2 g/\sigma$, where g is the magnitude of the acceleration due to gravity, is the gravitational Bond number that measures the relative importance of gravitational and surface tension forces. $Ca \equiv \mu u/\sigma$ is the capillary number that measures the relative importance of viscous and surface tension forces. $N_e \equiv (\epsilon R/\sigma)(U_0/H)^2$ is the electric Bond number that measures the relative importance of electrical and surface tension forces. $K \equiv \epsilon/\epsilon_o$ is the ratio of the

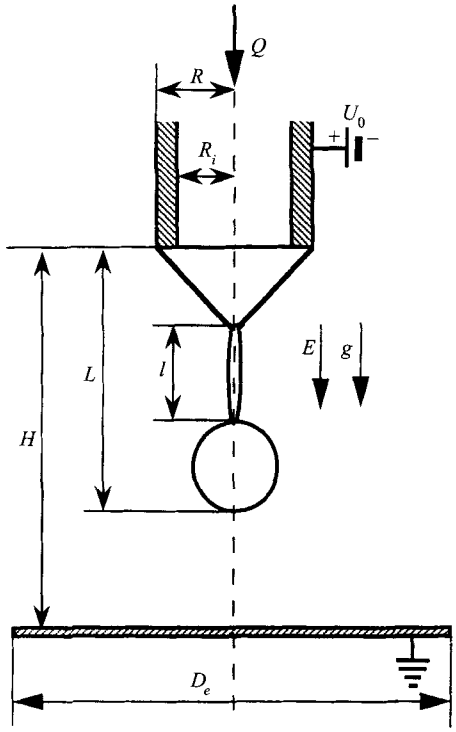

FIGURE 3. Schematic of a drop forming out of a capillary under an electric field and gravity.

permittivity of the drop to that of the ambient fluid. $Pe \equiv (\epsilon/\gamma)/(R/u)$ is the Péclet number that measures the relative importance of electrical relaxation time $\tau_e \equiv \epsilon/\gamma$ to the characteristic time for fluid motion $\tau_f \equiv R/u$. R_i/R and H/R are length ratios (cf. figure 3). This choice of dimensionless groups is of course not unique. For example, instead of the pair Re and G, one could equally well work with the pair We and St, where $We \equiv ReCa$ is the Weber number that measures the relative importance of inertial to surface tension forces and $St \equiv G/Ca$ is the Stokes number that measures the relative importance of gravitational to viscous forces.

In the absence of an electric field, the profile of a static pendant drop of fixed volume V is set by a single dimensionless group, the gravitational Bond number G (see e.g. Michael 1981). The dynamics of drop formation from a capillary in the absence of an electric field is governed by Re, Ca, and R_i/R in addition to G. Zhang & Basaran (1995) have presented a thorough study of the effects of Re, Ca, and R_i/R on the dynamics of drop formation in the absence of an electric field. For example, an increase in Reynolds number, which is typically caused in the experiments by increasing either the flow rate or the tube radius, leads to a larger elongation of the forming drop prior to breakup and increases the volume of the primary drop that results upon breakup. An increase in the capillary number, which is typically caused in the experiments by either increasing viscosity or decreasing surface tension, causes a significant increase in the thread length because of the enhancement of the damping of disturbances on the thread surface that is provided by the increase in the relative importance of viscous forces. A decrease in the relative importance of surface tension forces, however, results in a decrease in the volume of primary drops. The wall thickness (or the ratio of inner radius of the tube to its outer radius R_i/R) is

found to have a negligible effect on the dynamics if capillary tubes of sufficiently thin walls, $R_i/R > 0.4$, are used.

As shown above, the application of an electric field broadens the parameter space that governs the dynamics of forming drops. The effect of the electric Bond number N_e, for example, can be readily appreciated in the light of a simple physical system. If surface charge q is uniformly distributed on the surface of a conducting fluid sphere of radius R placed in an infinite expanse of an ambient dielectric fluid of the same density as the sphere, the pressure inside the sphere, p, would be related to that outside it, p_o, in the absence of viscous stresses due to fluid motion, as

$$\begin{aligned} p &= p_o + \left(\frac{2\sigma}{R} - \frac{1}{2}\epsilon_o E_n^{(o)2}\right) = p_o + \left(\frac{2\sigma}{R} - \frac{1}{2\epsilon_o}\sigma_E^2\right) \\ &= p_o + \frac{\sigma}{R}\left[2 - \frac{1}{2K}N_e\left(\frac{E_n^{(o)}}{U_0/H}\right)^2\right] \end{aligned} \tag{1}$$

where $E_n^{(o)}$ is the normal component of the electric field on the ambient fluid side of the interface, σ_E is the surface density of charge, and $\sigma_E \equiv q/4\pi R^2 = \epsilon_o E_n^{(o)}$. The first line of equation (1) makes it plain that increasing the local field strength or the local charge density reduces the effective electromechanical surface tension (cf. Miller & Scriven 1970) of the interface. The second line of (1) restates this fact in terms of the dimensionless group N_e which measures the importance of electrical force relative to that of surface tension force.

Were the drop a perfect conductor, $\tau_e = 0$. In that case, the entire drop surface would be an equipotential surface and the electric field inside the growing drop would vanish (see e.g. Melcher & Taylor 1969). When the drop liquid is not a perfect conductor, there will necessarily be a difference in electrical potential between the tip of the capillary and the apex of the growing drop. This potential drop ensures that the surface is subject to a tangential electric field. Moreover, if the drop is also not a perfect insulator, then its surface will support a distribution of free charge. When an interface supports both a tangential electric field and free surface charge, it is subject to an electrical shear stress that equals their product (cf. Melcher & Taylor 1969). In the absence of gradients in surface tension, such an electrical shear stress can only be balanced by a viscous shear stress exerted by the drop liquid on the interface. Such electrical shear stresses, aside from driving bulk circulations inside the growing drops, can also be expected to play a major role in stabilizing the liquid thread during its development and extension. Indeed, stabilization of fluid interfaces by electrical shear stresses has attracted much attention in the literature in studies of liquid jets (Taylor 1969; Saville 1970, 1971; Mestel 1994), electrostatic atomization (Hayati *et al.* 1986), and liquid bridges (Sankaran & Saville 1993).

Although the dimensionless groups listed in this section completely govern the response of a forming drop, one must be careful not to draw certain conclusions pertaining to the relative importance of competing effects based solely on their values. For example, when a drop is grown at an infinitesimally slow flow rate ($Re \ll 1$, $Ca \ll 1$) from a capillary in the absence of an electric field under the condition that $G \ll 1$, the drop shape will be a section of a sphere during the early stages of the drop growth (see e.g. Zhang & Basaran 1995). However, the smallness of G does not imply that the effect of gravitational force will remain negligible compared to that of surface tension force as the drop grows. Indeed, as the quantity $G^* \equiv G(V/R^3)^{2/3}$, which is an effective gravitational Bond number, gets large as the drop volume increases, the

drop shape will begin to deviate from a section of sphere and the drop will ultimately detach and fall from the capillary (cf. figure 1). Moreover, although viscous and inertial forces are unimportant throughout most of the formation process in this situation, they cannot be neglected inside the liquid thread during its rapid extension, thinning, and rupture. Similarly, during the period in which a thread forms and breaks in drop formation in the presence of an electric field (cf. figure 2), the characteristic time for fluid motion in the thread is not determined by R/u. In this case, the effective Péclet number that measures the relative importance of the electrical relaxation time and the effective process time may be several orders of magnitude larger than the Péclet number. Hence, if the electrical relaxation time is neither zero nor extremely small, the electric potential may vary along the charged surface of the liquid thread.

Although many parameters control the dynamics of drop formation in an electric field, this paper stresses primarily the effects due to an applied field whose strength is given by $E_0 \equiv U_0/H$. Two measures of interface deformation are convenient for describing the evolution in time of the shape of a growing drop and the dynamics of the liquid thread under an applied electric field. As shown in figure 3, these are the instantaneous length of the drop, L, and the instantaneous length of the liquid thread, l, both measured along the tube axis. In what follows, t refers to time measured from the instant of detachment of the previous drop. Moreover, throughout the remainder of the paper, the subscript d is affixed to L, l, and t to denote their values at the instant when the drop is about to detach and the superscript 0 is affixed to L, l, and volume V to refer to these quantities when they are measured in the absence of an electric field.

3. Experimental approach

The experiments have been designed to obtain quantitative information on the effects of varying the strength of an electric field on the evolution in time of the drop shape and the necking process that precedes drop detachment. Moreover, attention is also paid in the experiments to characteristics of satellite droplets that are generated subsequent to the breakup of the liquid thread.

3.1. *Apparatus*

The experiments are performed with a set-up which builds on our earlier study of drop formation in the absence of an electric field (Zhang & Basaran 1995), appropriately modified so that an electric field can be applied vertically. Because certain pieces of the apparatus and some of the experimental procedures are identical to those described by Zhang & Basaran (1995), this section briefly summarizes those features that are common to both papers and emphasizes new features.

The experimental apparatus consists essentially of a fine capillary tube through which the liquid is delivered at a constant volumetric flow rate by a liquid syringe pump (ATI Orion M361) and from the tip of which a liquid drop is formed or grown. The capillary tubes are made of stainless steel (Vici Valco Instrument Co.) and have tips that have been electropolished and machined flat to allow the drop liquid to wet completely the front surface and pin to the outer sharp edge of the tip.

The results to be reported in §4 have been obtained with the capillary tube arranged vertically above a grounded horizontal plate electrode which is made of copper and has a diameter of 15 cm. The tip of the capillary is located a distance $H = 3$ cm from the horizontal electrode. The capillary, which serves as the other electrode, is connected to a high-voltage DC power supply (Bertan Associates, Inc., Series 225) with

	μ (g cm^{-1} s^{-1})	σ (g s^{-2})	γ (ohm^{-1} cm^{-1})
Water	0.01	72.55	4×10^{-6}
0.1 mM NaCl	0.0101	72.73	1×10^{-3}
1 mM NaCl	0.0105	74.34	9×10^{-3}

TABLE 1. Physical properties of liquids and liquid–air interfaces in experiments.

a maximum current of 0.3 mA and variable voltage of 0–50 kV. A bottom electrode of a sufficiently large diameter relative to the diameter of the capillary is required to eliminate edge effects and ensure that the experimental results are independent of whether the capillary or the horizontal plate is the high-voltage (grounded) electrode. Moreover, the results reported in §4 are independent of the polarity of the applied electric field.

The capillary is immersed in a glass tank filled with the ambient fluid. The whole apparatus is placed on a vibration isolation table from Newport.

A piece of equipment that is essential to the present study is the ultra-high-speed video camera by Kodak (Ektapro Electronic Memory Motion Analyzer Model EM1012) for continuously capturing images of the drop formation process and associated hardware for recording, storing and analysing drop shape data. The camera system is composed of an intensified imager, which can record 1 000 full images or 12 000 partial images per second and allows rapid and accurate determination of the loci of instantaneous interface profiles from which the various measures of drop deformation, i.e. L and l, and drop volume are evaluated.

3.2. *Materials*

The drop liquids are either triple distilled water from Millipore Corp. or solutions of sodium chloride (NaCl) in distilled water. The physical properties of these systems are given in table 1. The viscosities and surface tensions of these fluids have been measured by a Cannon-Fenske viscometer and a pendant drop method (Harris & Byers 1989), respectively. These values agree well with those that have been published in the literature (Dean 1979). The conductivities have been measured by a conductance-resistance meter (YSI Model 34).

The aqueous NaCl solutions with different concentrations have been chosen because of their desirable physical properties, namely their viscosities and surface tensions are not too different from those of pure water, but their electrical conductivities can be made to vary by three orders of magnitude. Based on linear stability analyses of the effects of electrical shear stresses on the stability of liquid jets (Saville 1970, 1971; Mestel 1994), it is expected that large variations in conductivity can have a big impact on the evolution in time of the shapes of forming drops and, in particular, the dynamics of liquid threads.

3.3. *Procedures*

In a typical run, a steady flow with a desired rate is established through the capillary at an electric field of certain strength and the system is allowed to run for about 30 minutes before measurements are taken. A periodic flow situation is then reached in which the drops form, grow, and detach from the outlet of the capillary. Since in this dripping regime primary and satellite drops of uniform sizes are continuously created as verified in the experiments, the present technique provides a reliable and

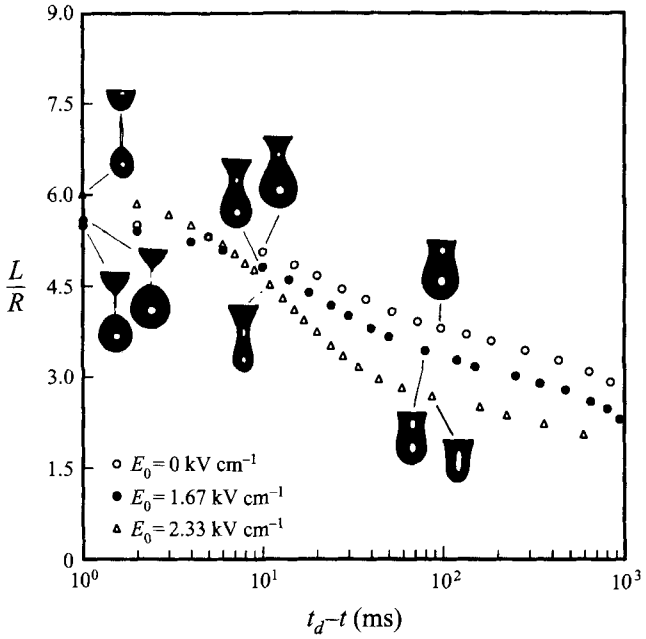

FIGURE 4. Evolution in time of the dimensionless length of water drops, L/R, growing out of a capillary of outer radius $R = 0.16$ cm at the liquid flow rate $Q = 1$ ml min^{-1} in the presence of an electric field of different strengths, where t_d is the time at the instant of drop detachment.

repeatable picture of the dynamics of drop formation. Reproducibility of results for drop shape and volume has been found to be within 5% by making measurements under the same conditions, but at different times. All experiments are performed at the room temperature of $22° \pm 0.5°$C.

4. Results and discussion

In order to study the effects of an externally applied electric field on the physics of drop formation — the development, extension, and breakup of the liquid thread and, subsequently, the generation of primary drops and the creation and dynamical behaviour of satellite droplets — a series of experiments has been performed by systematically varying one of the dimensional variables while holding all others fixed. In the experiments, physical and geometrical parameters have been varied in such a way that $0.33 \leqslant Re \leqslant 66.31$, $9.04 \times 10^{-6} \leqslant Ca \leqslant 3.62 \times 10^{-3}$, $8.71 \times 10^{-2} \leqslant G \leqslant 3.48 \times 10^{-1}$, $K \approx 80$, $1.02 \times 10^{-10} \leqslant Pe \leqslant 1.84 \times 10^{-4}$, and $0 \leqslant N_e \leqslant 0.86$. Most of the results to follow on drop elongation L, thread elongation l, and volume of primary drops V are presented in dimensionless form by scaling their values by those measured in the absence of an electric field to emphasize the role played by an electric field in the formation dynamics.

4.1. *Drop elongation and breakup*

Figure 4 presents the entire history of the deformation of three growing drops of water that are each subjected to an electric field of different strength. In figure 4, the deformation history is presented quantitatively in terms of the drop length, L, non-dimensionalized by the outer radius of the capillary, R, as a function of *time measured backward from the moment when the drop just detaches* $t_d - t$. In the three situations

that are depicted in figure 4, the liquid flow rate and the outer radius of the capillary are $Q = 1$ ml min^{-1} and $R = 0.16$ cm, respectively. The relative time $t_d - t$ emphasizes the period during which the growing pendant drop necks and breaks. Simply stated, $t_d - t = 0$ stands for the instant of drop detachment and the point in each data set for which $t_d - t$ is largest corresponds to the smallest value of the dimensionless elongation L/R that is measured at the beginning of the drop growth process. Evidently, the evolution in time of the drop shape and elongation are qualitatively similar regardless of the value of the strength of the electric field provided that the mechanism of drop formation is through dripping. Initially, as the volume of the drop increases due to the continuous supply of the drop liquid through the capillary, the drop deforms slowly under the action of electrostatic and/or gravitational forces. At long times, however, the volume of the drop becomes sufficiently large that the increase of electrostatic and/or gravitational forces over surface tension force causes a large portion of the drop to fall rapidly. In the meantime, a liquid thread, which connects the bottom portion of the drop to the liquid cone hanging from the capillary, develops, elongates rapidly, and eventually breaks up (cf. figure 1 and Zhang & Basaran 1995). The elapsed time during the latter stage of drop formation is much shorter than the former one and depends weakly on the field strength with a time scale of $t_d - t$ less than about 100 ms.

The results and trends depicted in figure 4 can be rationalized as follows. First, on account of the fact that the effective electromechanical tension of the interface falls as the strength of the electric field increases as discussed in §2, it accords with intuition that the volume of primary drops decreases significantly and the frequency of drop production increases when the strength of the applied electric field increases, as shown by the photograph inserts to figure 4. Second, these inserts also show that toward the end of the first stage of drop formation, $t_d - t \approx 100$ ms, whereas the drops are pear-shaped when the field strength is zero or weak, they are nearly spheroidal when the field strength is large. To reconcile this observation with intuition, one can imagine placing a conducting fluid sphere in an infinite expanse of an ambient dielectric fluid of the same density as the sphere and subjecting the drop to a uniform electric field whose strength equals E_0 infinitely far from the sphere. In this case, a charge density is induced on the surface of the sphere such that it varies with the polar angle measured from a pole of the sphere as $\sigma_E = 3\epsilon_o E_0 \cos\theta$ (see e.g. Reitz & Milford 1967). Thus, each point on the surface of the sphere would be subjected to an outwardly pointing normal electrical stress that equals $\sigma_E^2/2\epsilon_o$. These electrical stresses would tend to deform the drop into a spheroid in the direction of the applied field as the importance of the electrical force relative to that of the surface tension force increases. Figure 4 also shows that whereas for $t_d - t > 100$ ms, $(L/R)_{E_0=2.33\text{kV cm}^{-1}} < (L/R)_{E_0=1.67\text{kV cm}^{-1}} < (L/R)_{E_0=0\text{kV cm}^{-1}}$, at $t = t_d$, $(L_d/R)_{E_0=1.67\text{kV cm}^{-1}} < (L_d/R)_{E_0=0\text{kV cm}^{-1}} < (L_d/R)_{E_0=2.33\text{kV cm}^{-1}}$. This is because at breakup the limiting length of the drop, L_d, equals the sum of the height of the liquid cone, the limiting length of the thread, l_d, and the effective diameter of the about-to-form primary drop. Whereas the first of these changes little, the second one increases and the third one decreases as the field strength increases (see also figures 5–8 below).

It is noteworthy that since the volume of primary drops decreases as the field strength increases, the increase that is observed in the limiting elongation L_d/R of water drops forming in an electric field of sufficiently large strength is attributable to an increase in thread length. Moreover, the concurrent increase in drop elongation that results at breakup and decrease in the volume of primary drops that are produced

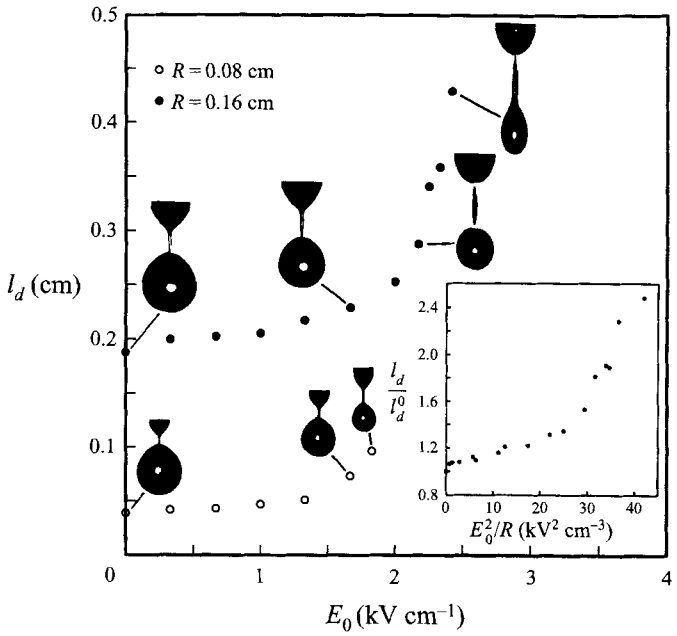

FIGURE 5. Limiting length of liquid threads of water drops, l_d, as a function of the field strength E_0 for capillaries of two different sizes at the liquid flow rate $Q = 1$ ml min^{-1}. Insert: Dimensionless limiting length of liquid threads of water drops, l_d/l_d^0, which is defined as the ratio of the thread length measured at the instant when the drop is about to detach in the presence of an electric field to that measured in the absence of an electric field, as a function of E_0^2/R.

upon breakup at high field strengths greatly affect the dynamics of thread rupture and the subsequent generation and fate of satellite droplets. These are all issues that are returned to in what follows.

4.2. *The liquid thread*

Figure 5 shows that the limiting thread length l_d of water drops increases monotonically with the strength of the applied electric field E_0. Here results are shown for two different capillaries of $R = 0.08$ and 0.16 cm, but the flow rate is held fixed in both situations at $Q = 1$ ml min^{-1}. The increase in the limiting thread length with increasing electric field strength becomes more pronounced as field strength becomes large, in particular when $E_0 > 1.5$ kV cm^{-1}. This increase in the limiting length of the thread at large field strengths results in an increase in the volume of satellite droplets that form subsequent to thread breakup, a point that is returned to in §4.3.

Harris & Basaran (1993) have shown that the manner in which surface charge distributes on the surface of an electrified pendant drop is a strong function of the length of the tube from which it is hanging. If the drop is emanating from a hole of radius R on the top plate of a parallel-plate capacitor the faces of which are separated by a distance H, i.e. the situation in which the tube length is zero, surface charge density scales as U_0/H. On the other hand, if the drop is hanging from a tube that is attached to the top plate of the capacitor and the tube is much much longer than the distance between the tip of the tube and the bottom plate, i.e. the top plate is effectively at infinity as in this paper, surface charge density then scales as U_0/R. Therefore, the ratio of electrical force to surface tension force scales as $\mathcal{N}_e \equiv (\epsilon/\sigma)(U_0^2/R) = (\epsilon H^2/\sigma)(E_0^2/R)$. Thus, at the same value of the applied field

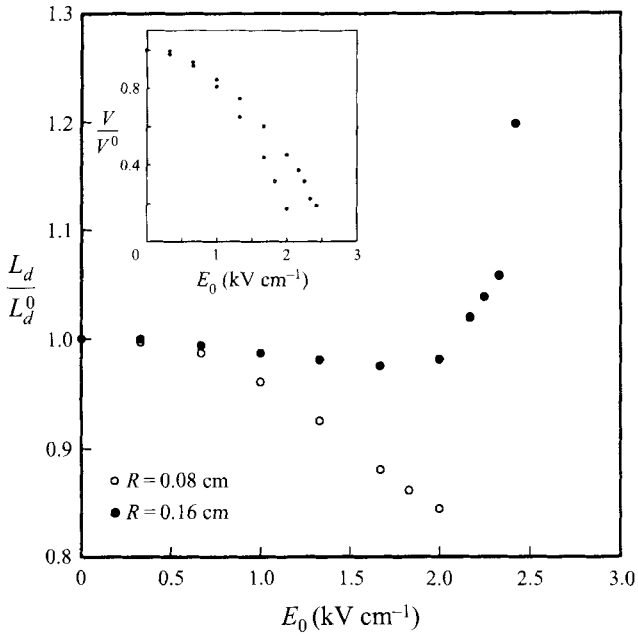

FIGURE 6. Dimensionless limiting length of water drops, L_d/L_d^0, as a function of the field strength for capillaries of two different sizes at the liquid flow rate $Q = 1$ ml min^{-1}. The insert shows the dimensionless volume of primary drops, V/V^0, under identical conditions.

strength, the thread length made dimensionless with the limiting thread length l_d^0 in the absence of field, namely l_d/l_d^0, should increase as the tube radius decreases. Equivalently, to achieve the same value of the dimensionless limiting thread length, the larger the capillary radius the larger is the field strength that would be required. In other words, the variation of l_d/l_d^0 with E_0^2/R should be virtually independent of R, a result that is confirmed by the insert to figure 5. Moreover, since the volume of the primary drop decreases with increasing field strength, the primary drop accelerates faster in a higher field and the filament thereby reaches a greater length before disturbances on it can reach a size sufficient to rupture it.

Although the limiting thread length l_d increases dramatically with the field strength E_0 when E_0 is sufficiently large as shown in figure 5, the drop length, which is the composite of the thread length and essentially the effective diameter of the primary drop that will be formed once the thread breaks, varies in a complex manner with E_0 that depends on the radius of the capillary. Figure 6 depicts the variation of the limiting drop length relative to that at zero electric field strength, L_d/L_d^0, with the applied field strength E_0. As discussed earlier in the context of figure 4, the drop length is determined by the competition between the decrease in the size of the primary drop on the one hand and the increase in the length of the thread with increasing field strength. The insert to figure 6 shows that the rate at which the relative volume of the primary drop V/V^0 falls with rising field strength increases as R decreases. Therefore, given the relatively small increase in the limiting length of the thread and the considerable reduction in the size of the primary drop, figure 6 shows that the limiting length of the drop forming from a capillary of $R = 0.08$ cm decreases monotonically as the strength of the applied electric field increases. By contrast, with a competition between a rapidly increasing thread length and a moderately decreasing volume of the primary drop, the limiting drop length when

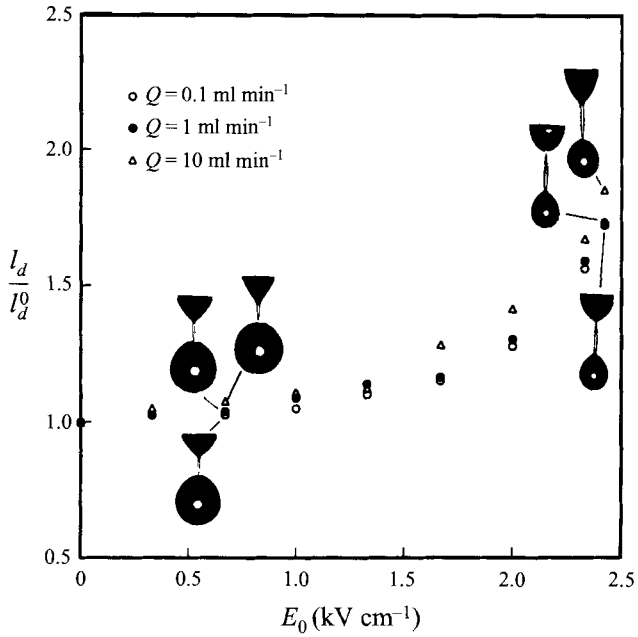

FIGURE 7. Dimensionless limiting length of liquid threads of water drops, l_d/l_d^0, which is defined as the ratio of the thread length measured at the instant when the drop is about to detach in the presence of an electric field to that measured in the absence of an electric field, as a function of the field strength at different liquid flow rates for a capillary of $R = 0.16$ cm.

$R = 0.16$ cm decreases slightly at low field strengths, attains a minimum at $E_0 \sim 1.7$ kV cm^{-1}, and then increases dramatically with E_0 at high field strengths.

Figure 7 shows the variation of the dimensionless limiting length of threads, l_d/l_d^0, with the strength of the applied electric field for water drops forming from a capillary of $R = 0.16$ cm at three different flow rates. Although the thread length increases as the field strength increases in each case, the enhancement of the elongation of the thread clearly depends on the flow rate. In the absence of electric field, Zhang & Basaran (1995) have shown that the length and diameter of liquid threads change little with increasing flow rate at low flow rates ($Q \leqslant 1$ ml min^{-1}) but the thread length increases greatly and the thread thickness increases moderately with Q at high flow rates. It accords with intuition that whereas the process time decreases with increasing flow rate, the growth rate of disturbances that rupture the thread should remain virtually independent of flow rate to a first approximation. Thus, the dimensionless limiting length of threads should increase with increasing flow rate.

Figure 8 shows the variation of the volume of primary or breakoff drops normalized by their value at zero field strength, V/V^0, with applied field strength E_0. As in figure 7, the results shown are for water drops forming from a capillary of $R = 0.16$ cm at the flow rates of $Q = 0.1$, 1, and 10 ml min^{-1}. The general trend that the volume of primary drops falls as field strength increases accords with results presented in the previous paragraphs and also with those of other researchers (see e.g. Byers & Perona 1988). However, the variation of the normalized volume of primary drops with flow rate at a fixed value of the applied field strength is more complex. The amount of surface charge that a forming drop bears falls as the flow rate, or the dripping

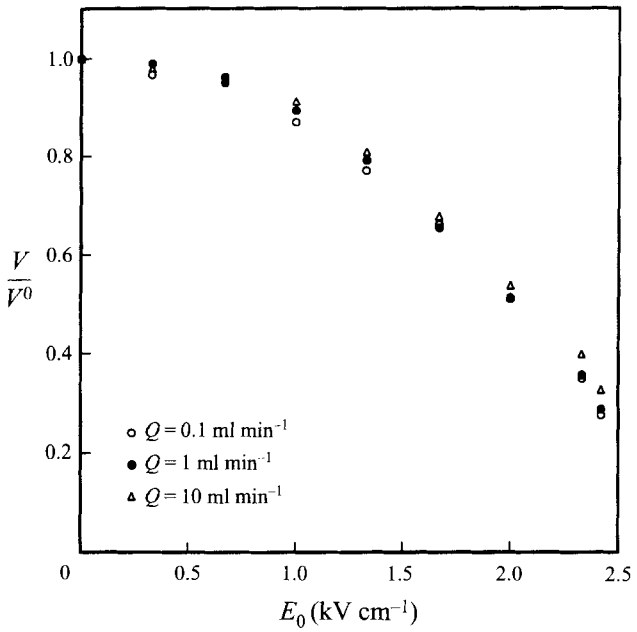

FIGURE 8. Dimensionless volume of primary drops of water, V/V^0, which is defined as the ratio of the volume of the primary drop in the presence of an electric field of a certain strength to that measured in the absence of an electric field, as a function of the field strength at different liquid flow rates for a capillary of $R = 0.16$ cm.

frequency, rises. Thus the larger the flow rate the larger is the effective surface tension of the drop and the greater is the normalized volume of the primary drop.

Figure 9 illustrates the effect of electrical conductivity on the variation of the relative limiting length of threads with applied field strength while holding both the flow rate and the capillary radius fixed at $Q = 1$ ml min^{-1} and $R = 0.16$ cm, respectively. Figure 9 makes plain that when subjected to an electric field of the same strength, the limiting length of the thread falls as the conductivity of the liquid or the concentration of NaCl in distilled water rises. For the NaCl solutions studied, the electric relaxation times τ_e are extremely short – 8×10^{-10} s $\leqslant \tau_e \leqslant 7 \times 10^{-9}$ s – compared to that for distilled water – $\tau_e \approx 1.7 \times 10^{-6}$ s. To investigate whether charge relaxation could be a factor in the thread during its rapid stretching prior to its rupture, the electrical relaxation time needs to be compared to the characteristic time for fluid motion, τ_f.

For water drops under an applied field of strength $E_0 = 2.33$ kV cm^{-1}, at $t_d - t \approx 3$ ms the stretching rate of the thread $\mathring{l}$ is about 25 cm s^{-1} when the thread radius r is about 1/50th of the tube radius or about 3.2×10^{-3} cm. Thus, at this instant in time $r/\mathring{l}$ is about 1.3×10^{-4} s. Recent calculations by Zhang, Padgett & Basaran (1996) on stretching liquid bridges have shown that the average axial velocity of the fluid in parts of a water bridge can attain values on the order of 100 times the stretching rate at this value of the thread radius. Therefore, $\tau_f \approx 10^{-6}$ s at this point in time and it decreases as the thread continues to get thinner. The value of τ_f for the drops of NaCl solutions is roughly the same as that of water drops. Because the electrical relaxation times are about three orders of magnitude shorter than the characteristic times for fluid motion for drops of NaCl solutions, any free charges that might initially be brought into the interior of the threads of

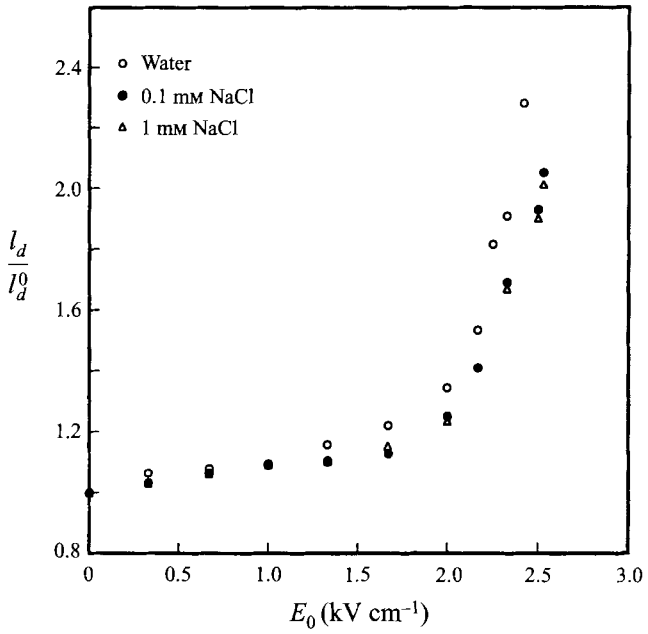

FIGURE 9. Dimensionless limiting length of liquid threads, l_d/l_d^0, which is defined as the ratio of the thread length measured at the instant when the drop is about to detach in the presence of an electric field to that measured in the absence of an electric field, as a function of the field strength for solutions of different concentrations of NaCl and water flowing out of a capillary of $R = 0.16$ cm at a liquid flow rate of $Q = 1$ ml min^{-1}.

such drops by the electric field will quickly migrate to and accumulate at the fluid interface where there is a discontinuity in electrical conductivity (see e.g. Melcher & Taylor 1969). Hence, the electric field everywhere inside such drops, including the thread, would be extremely weak compared to the field outside them. Therefore, although surface charges would be present on the interfaces of growing drops of NaCl solutions, because of the smallness of the tangential component of the electric field on their interfaces, the electric stresses would act virtually in a direction normal to the drop surfaces. Therefore, the increase in l_d/l_d^0 with E_0 observed for such highly conducting drops is due essentially to the enhancement of the elongation of the drop along its axis of symmetry with increasing field strength. By contrast, τ_f can become comparable in magnitude to τ_e within the threads of drops of distilled water and thus charge relaxation effects cannot be neglected during the latter stages of their breakup. Evidently, the small but finite electric shear stresses that act on the surfaces of water drops are enough to enhance the stability of and increase the elongation of their liquid threads. The argument given here that electrical shear stresses play a role in delaying the rupture of threads of drops of distilled water but not of drops of NaCl solutions can be strengthened by carrying out experiments at values of the field strength slightly exceeding those shown in figure 9 where the mode of drop formation changes from dripping to jetting. These experiments have shown that whereas it is possible to attain stable cone-jets with distilled water, it is not possible to do so with NaCl solutions. These results accord with those of Hayati *et al.* (1986) and others that electrical shear stresses must be present if the cone-jet mode is to be attained.

Whereas the conductivity of water can be increased by a factor of 250 by dissolving 0.1 mM of NaCl in it, the conductivity of a 1 mM NaCl solution in water is only 9

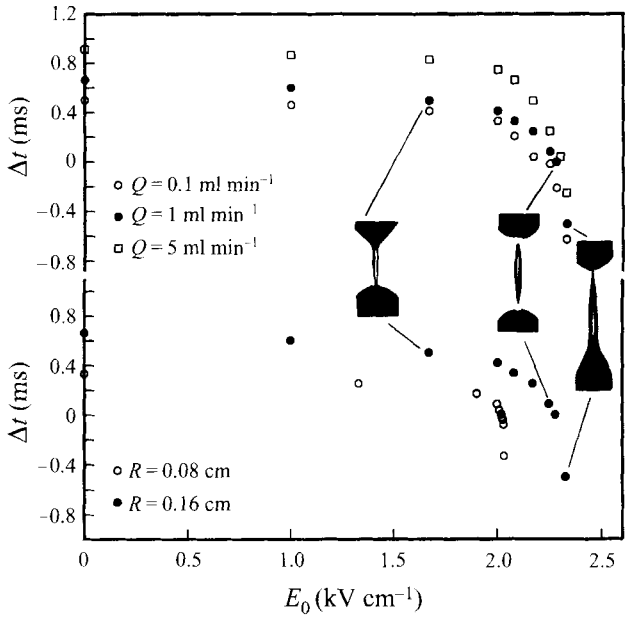

FIGURE 10. Variation of the interaction time, Δt, with field strength for water drops flowing out of a capillary of a fixed radius of $R = 0.16$ cm at three liquid flow rates, top, and for water drops flowing out of capillaries of different radii at a fixed liquid flow rate of $Q = 1$ ml min^{-1}, bottom.

times that of a 0.1 mM NaCl solution (cf. table 1). Therefore, as shown in figure 9, it is not too surprising that at the same value of the applied field strength the difference in the limiting thread length between the drops of the two NaCl solutions is small compared to that between the drops of NaCl solutions and the drops of water.

As $t \rightarrow t_d$, the liquid thread is rapidly stretched by the the downwardly accelerating bottom globular portion of the drop. Indeed, within a time period on the order of a millisecond, the liquid thread breaks at its downstream end from what will become the primary drop and at its upstream end from a virtual liquid cone that will remain pendant from the capillary. The issue of what happens to the thread once it is free is taken up below in §4.3. The issue that is of interest here is the manner in which the thread breaks. In the absence of an electric field (cf. Zhang & Basaran 1995) and when the field strength is small, the thread consistently breaks first at its downstream end due to the larger capillary pressure that develops there on account of the larger curvature of the interface (Zhang & Basaran 1995). However, as the field strength increases, the volume of the portion of the growing drop that is the precursor of the primary drop continuously decreases while that of the liquid cone remains virtually unchanged. When the volume of the precursor of the primary drop falls below a certain amount, the zone of highest curvature switches from the lower end of the liquid thread to its upper end. Hence, the thread breaks first at its upper end when the field strength becomes sufficiently large, which was heretofore not known. Evidently, at a critical value of the field strength, the thread breaks at its two ends simultaneously, as shown by the photograph inserts to figure 5.

This switch in the breakup sequence can be clearly demonstrated by plotting the variation of the interaction time, which is defined as the elapsed time between the breakup of the lower end of the thread and that of its upper end, Δt, with the applied field strength. With this convention, a positive (negative) value of the interaction time

implies that the thread breaks first at its lower (upper) end. Figure 10 shows the variation of Δt with E_0 as a function of either the flow rate (at the top) or the capillary radius (at the bottom) for water drops forming out of capillaries. Figure 10 makes plain that the interaction time changes from positive to negative as the field strength increases regardless of the value of the flow rate or the capillary radius. Figure 10 also shows that the field strength required for reversing the sequence of breakups of the ends of the thread increases as the flow rate of the liquid or the capillary radius increases. The subtle effect of the electric field on the breakup mechanism of the liquid thread has important ramifications on the fate of satellite drops that are formed subsequent to its breakup.

4.3. *Satellite droplets*

Regardless of whether an electric field is applied, satellite droplets are observed to be created in most experiments directly as a result of the breakup of liquid threads. The electric field has three primary effects on the formation and fate of satellite droplets. These are (i) to control the volume of satellite droplets by varying the size of liquid threads; (ii) to switch the sequence of breakup of the two ends of the thread, and hence to change the initial direction of motion – upward or downward – of the satellite droplets; and (iii) to modify the distribution of surface charge on the satellite droplets, the primary drop, and the liquid cone that is left hanging on the capillary following the rupture of both ends of the thread.

Figure 11 shows four series of several photographs for a close look at thread breakup and creation of satellite droplets. These sets of photographs have been obtained during the formation of water drops from a capillary of $R = 0.16$ cm at the flow rate of $Q = 1$ ml min^{-1} but with each set under an electric field of different strength. The sequence of photographs shown in any given series has been obtained at irregular times. The black area visible at the top of each photograph corresponds to a portion of the liquid cone hanging from the capillary tube. It moves up and down in a given sequence because the surface of the liquid cone oscillates during the latter stages of and subsequent to thread breakup. The black area visible at the bottom of each photograph corresponds to a portion of the primary drop that forms upon thread breakup. The white circle that is visible at the base of some of the photographs is the reflection of the light used in illuminating the drop. When the strength of the electric field equals zero or is low, a thread consistently breaks first at its downstream end, which leads to the formation of the primary drop, as shown in figure 11(*a–c*). Immediately after the thread breaks at its downstream end, the now freed end of the thread is accelerated in the upward direction by the unbalanced force of surface tension (Peregrine *et al.* 1990; Zhang & Basaran 1995). Soon thereafter, the thread breaks again but this time at its upstream end. As its ends rapidly approach one another, the thread tends toward a sphere to form a satellite droplet that is now completely separated from both the detached primary drop and the pendant liquid cone hanging from the capillary. Once a satellite droplet is created in this manner, driven by the unbalanced force of surface tension acting at its lower end, it tends to move upward toward the liquid cone hanging from the tube.

By contrast, when the strength of the electric field is sufficiently high, as in figure 11(*d*), reversing the order in which the ends of the thread break causes a downward net force on the satellite droplet right after it is generated due to the downward-acting unbalanced force of surface tension. This force, coupled to the gravitational force acting on it, drives the satellite droplet in the downward direction toward the falling primary drop. When the satellite droplet gets sufficiently close to the primary

(*a*) $E_0 = 0$

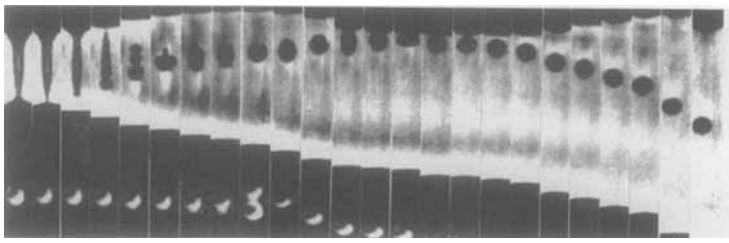

(*b*) $E_0 = 0.5$ kV cm^{-1}

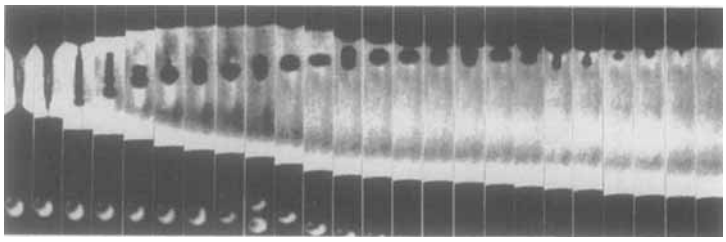

(*c*) $E_0 = 1$ kV cm^{-1}

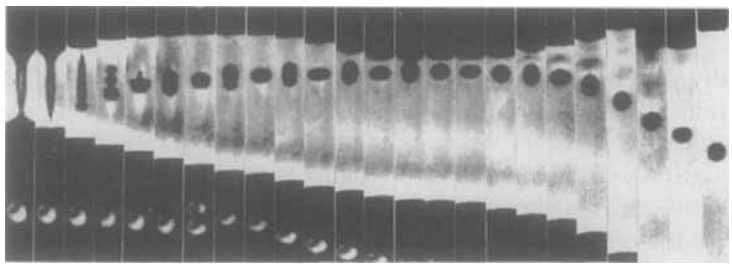

(*d*) $E_0 = 2.33$ kV cm^{-1}

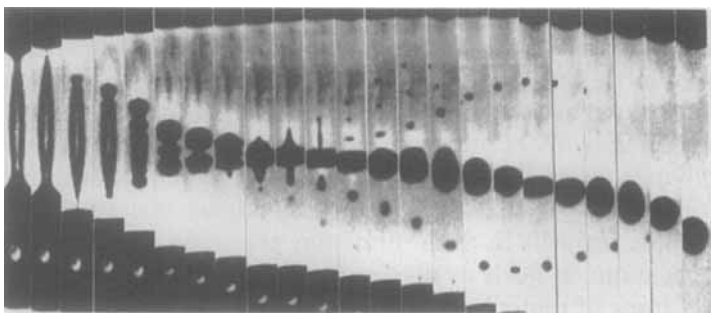

FIGURE 11. Time sequences of photographs depicting the breakup of liquid threads and the creation and fate of satellite droplets in the situations in which water is flowing out of a capillary of $R = 0.16$ cm at $Q = 1$ ml min^{-1} under an electric field of four different field strengths.

drop, it is repelled by the primary drop due to both drops bearing large amounts of net surface charges of the same sign. Under the repulsive force it experiences from both the primary drop and the liquid cone that is hanging from the capillary, the satellite droplet moves back forth between the liquid cone and the primary drop,

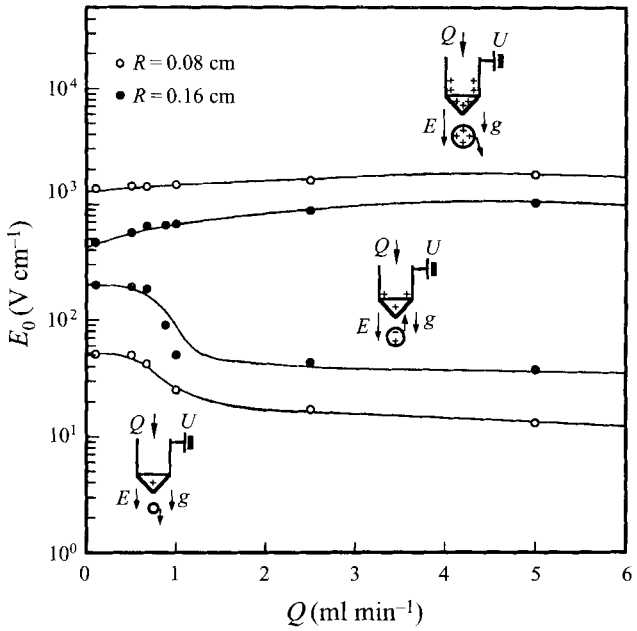

FIGURE 12. Operating diagram depicting the response of satellite droplets of water following thread breakup as functions of field strength and liquid flow rate for capillaries of two different sizes.

and eventually is deflected away from the axis of symmetry. Thereafter, the satellite droplet migrates downward as an isolated liquid mass.

The dynamical response of a satellite droplet is complicated but depends on the initial deformation and the manner of breakup of the liquid thread before its creation on the one hand and the electrostatic and gravitational forces it is subjected to after its creation on the other hand. As shown by Zhang & Basaran (1995), when a liquid drips from a capillary in the absence of an electric field, the satellite drops can be eliminated by merging – coalescing – them with the liquid cone hanging from the capillary *only* when the capillary has a sufficiently small radius. With capillaries of moderate radii, although the satellite droplets tend to move upward initially, they collide with and bounce off the surface of the liquid cone. Thereafter, such satellites move downward as isolated free droplets, as shown in figure 11(*a*). However, when an electric field of low strength is applied, satellite droplets formed from such capillaries are observed to consistently be attracted by and coalesce with the liquid cones hanging from the capillaries, as shown in figure 11(*b*). Therefore, application of an electric field of the right strength offers a heretofore unknown means for controlling and eliminating satellite droplets in drop formation processes. This discovery could have important applications in fields as diverse as separations, ink-jet printing, and spray coating, where drops of uniform sizes are required.

Figure 12 summarizes quantitatively the response of satellite droplets of water in an electric field. Figure 12 shows that depending primarily on the strength of an electric field, there exist three distinct regions of satellite droplet response. At the two extremes of field strength – very low and very high – satellite droplets end up as isolated liquid masses that ultimately move in the downward direction. By contrast, in the region of moderate field strengths, satellite droplets are eliminated by being attracted to and coalescing with the pendant liquid cone hanging from the capillary after they approach the conical meniscus. The data points in figure 12 define

boundaries in parameter space that separate the region in which a satellite droplet is attracted to and coalesces with the pendant liquid cone from those regions in which a satellite droplet ends up as a separate entity. The uncertainty in the values of the field strength separating these regions is less than 5%.

It is at first sight puzzling that the satellite droplet should be attracted to and coalesce with, rather than be repelled by, the liquid cone since they both bear net surface charges of the same sign. However, when the field strength is low, the satellite droplet is created after the breakup of a short thread of small size or volume. Thus, although the satellite droplet bears a net surface charge which is of the same sign as that carried by the liquid cone, the amount of this charge is small. The applied field, however, also leads to the creation of induced charges on the surface of both the satellite droplet and the liquid cone. Evidently, when the satellite volume and the amount of net charge that it bears are low, the density of charge that is induced by the externally applied field on the surface of the satellite dominates over the net charge. Hence, as shown in the insert to figure 12, the surfaces of the satellite and the cone that face each other bear charges of different signs and the two liquid bodies attract each other. This reasoning accords with similar physical situations that arise in studies of electric-field-induced coalescence of liquid drops (Zhang, Basaran & Wham 1995; see also Davis 1964) and the interaction between supported liquid columns in an electric field (Feng & Basaran 1995). In the latter study, the authors show by computational experiments that two supported liquid columns bearing net charges of the same sign can be made to attract each other under the action of an externally applied electric field provided one of the columns carries a small amount of charge while the other carries a large amount of charge. In the present experiments, the analogue of the slightly charged column is the satellite and that of the highly charged column is the combination of the conical pendant drop that remains on the tube and the capillary.

Therefore, it follows from the discussion given in the previous paragraph that as the strength of the electric field exceeds a critical value, the net charge on a satellite droplet can attain a large enough value to dominate over the charge induced on it by the applied electric field. Hence even if the unbalanced force of surface tension that results upon thread breakup is able to bring the satellite droplet very close to the liquid cone, the charges of the same sign on the two liquid surfaces are enough to cause the two liquid masses to repel each other. Figure 11(*c*) shows that this is indeed the case when the field strength is increased from 0.5 to 1 kV cm^{-1}: the net charge effect is strong enough so that the satellite drop rebounds and moves in the downward direction as a separate droplet. Furthermore, if the field strength is increased even further, the thread breaks first at its upstream end as discussed earlier. In this case, the combination of the downward-acting unbalanced force of surface tension and the repulsion between net charges on the satellite droplet and the liquid cone are sufficient to render impossible the elimination of the satellite droplet by absorbing it into the liquid cone, as shown in figure 11(*d*).

Figure 12 shows that as the capillary size decreases, the range of field strengths over which the satellite droplet coalesces with the liquid cone, or the satellite droplet can be eliminated, increases. This is not too surprising on account of the finding by Zhang & Basaran (1995) that when the radius of the capillary is sufficiently small, satellite drops will readily coalesce with the liquid cone in the absence of electric field. Figure 12 also shows that flow rate has a negligible effect on the behaviour of satellite drops in an electric field unless it is very low, namely $Q < 1$ ml min^{-1}. At very low flow rates, the chances of eliminating the satellite droplet by using an electric

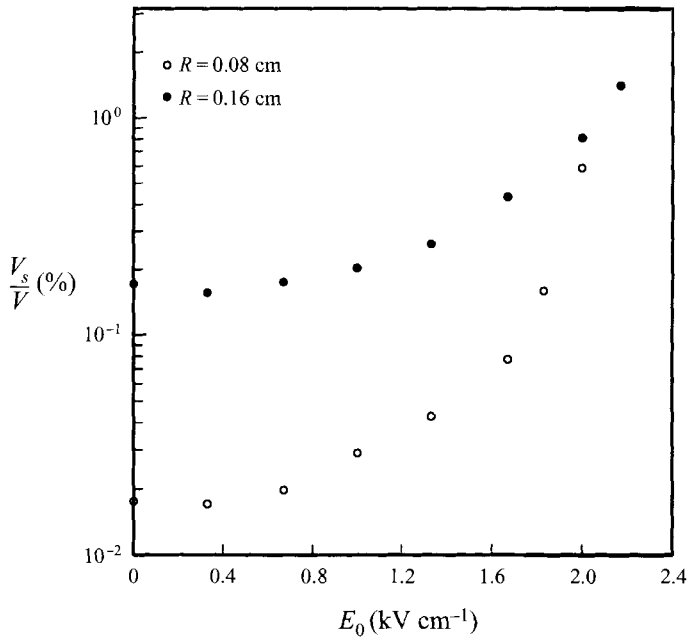

FIGURE 13. Dimensionless volume of satellite droplets of water, V_s/V, as a function of the field strength for capillaries of two different sizes at the liquid flow rate $Q = 1$ ml min^{-1}.

field become smaller and occur only over an extremely limited range of electric field strengths.

Figure 13 shows the variation of the volume of satellite drops with the strength of the applied electric field for drops of water that are formed at the flow rate of $Q = 1$ ml min^{-1} from two different capillaries, one with a radius of $R = 0.08$ cm and the other with a radius of $R = 0.16$ cm. Here the volume of the satellite droplets, V_s, is non-dimensionalized by the volume of their primary drops, V, at the same value of the field strength. Whereas the volume of primary drops decreases with increasing field strength (cf. figure 8), figure 13 makes plain that the volume of the satellite drops increases with increasing field strength on account of the increase in size of the liquid threads (cf. §4.2). Indeed, the volume of satellite droplets attain values exceeding 1% of that of the primary drops at the extremes of field strength attainable in the dripping mode. Of course, as the field strength continues to increase beyond this point, droplets are ejected from the apex of a pendant liquid cone in the jetting mode and the distinction between primary and satellite drops becomes blurred (Bailey 1988).

Figure 13 also shows that the rate at which the relative volume of satellites increases with field strength is larger for the smaller capillary. It is noteworthy that when the volume of a satellite droplet becomes sufficiently large due to an electric field of large strength, once the thread gives birth to the satellite the latter breaks one or more times to create one or more secondary satellites, as shown in figure 11 (*d*) or by Taylor (1964). In general, the secondary satellite droplets are much smaller in size, or volume, than the main one and, therefore, are ignored in the calculation of the volume of main satellite droplets. Once the secondary satellite droplets are created, they immediately move away from the main one and the axis of symmetry due to

the three-dimensional, large-amplitude oscillations that they undergo and the strong repulsion that they feel from each other.

5. Concluding remarks

Past studies of drop formation in an electric field had focused on such gross features of the process as the reduction in the volume of primary drops that results as field strength increases. In this paper, results of a detailed study are reported that focuses on issues such as the dynamics of liquid threads and the generation and fate of satellite droplets by taking advantage of an ultra-high-speed video camera. Through such studies, it has been uncovered here that whereas the thread always breaks first at its downstream end when the field strength is low, it breaks at its upstream end first when the field strength exceeds a critical value. Such insights into these and other mechanisms of breakup of liquid threads are essential in formulating a rational understanding of the fate of satellite droplets that form upon thread breakup. It has also been discovered that a weak electric field always causes a satellite droplet to coalesce with the liquid cone that is hanging from the capillary, a finding that should prove useful in the control and elimination of satellite droplets that are often undesirable in applications.

In spite of the fact that surfactants are commonly used in practical applications involving drop formation, their influence, which is due to interfacial tension variations and/or interfacial viscosity, remains largely unexplored. In studies of the formation of a drop of a surfactant-laden liquid from a capillary, the tension at the freshly formed interface of the drop may be quite different from the equilibrium or static value and may vary as a function of time in a manner dictated by the distribution of the surfactant on the expanding surface of the drop (Zhang, Harris & Basaran 1994). It has been learned through recent studies that dynamic surface tension plays a large role in modifying the physics of the formation of drops of surfactant-laden liquids in the absence of electric fields, in particular when the flow rate is sufficiently high (Zhang & Basaran 1995). There is also a need to develop an understanding of the effects of an externally applied electric field on the dynamics of drops of surfactant-laden liquids during their formation. It is expected that the presence of an electric field may disturb the surfactant distribution on the drop surface and change the local effective surface tension along the drop surface (Chang & Berg 1985), giving rise to a competition between flows induced by surface tension gradients and ones induced by electric shear stresses to radically alter the dynamics of the drop formation process.

This research was supported by the Division of Chemical Sciences, Office of Basic Energy Sciences, US Department of Energy under contract DE-AC05-96OR22464 with Lockheed Martin Energy Research Corp. (XZ, OAB), New Directions in Chemical Engineering Program of the School of Chemical Engineering and its Industrial Partners (OAB), and the Exxon Education Foundation (OAB). The authors thank Dr M. T. Harris of Oak Ridge National Laboratory for his thoughtful comments and suggestions on this work.

REFERENCES

BAILEY, A. G. 1988 *Electrostatic Spraying of Liquids.* Research Studies Press Ltd., Taunton, England.

BASARAN, O. A. & SCRIVEN, L. E. 1982 Profiles of electrified drops and bubbles. In *Proc. 2nd Intl Colloq. on Drops Bubbles* (ed. D. H. Le Croissette). Jet Propulsion Laboratory, Pasadena, California.

BASARAN, O. A. & SCRIVEN, L. E. 1990 Axisymmetric shapes and stability of pendant and sessile drops in an electric field. *J. Colloid Interface Sci.* **140**, 10–30.

BYERS, C. H. & PERONA, J. J. 1988 Drop formation from an orifice in an electric field. *AIChE J.* **34**, 1577–1580.

CHANG, L. S. & BERG, J. C. 1985 The effect of interfacial tension gradients on the flow structure of single drops or bubbles translating in an electric field. *AIChE J.* **31**, 551–557.

CLOUPEAU, M. & PRUNET-FOCH, B. 1990 Electrostatic spraying of liquids: Main functioning modes. *J. Electrostatics* **25**, 165–184.

DAVIS, M. H. 1964 Two charged spherical conductors in a uniform electric field: Forces and field strength. *Q. J. Mech. Appl. Maths* **17**, 499–511.

DEAN, J. A. 1979 *Lange's Handbook of Chemistry*. McGraw-Hill.

EGGERS, J. & DUPONT, T. F. 1994 Drop formation in a one-dimensional approximation of the Navier–Stokes equation. *J. Fluid Mech.* **262**, 205–221.

FENG, J. Q. & BASARAN, O. A. 1995 Interactions between two electrified liquid columns pinned on a dielectric solid surface. *Phys. Fluids* **7**, 667–679.

FERNANDEZ DE LA MORA, J. & LOSCERTALES, I. G. 1994 The current emitted by highly conducting Taylor cones. *J. Fluid Mech.* **260**, 155–184.

FILLMORE, G. L., BUEHNER, W. L. & WEST, D. L. 1977 Drop charging and deflection in an electrostatic ink jet printer. *IBM J. Res. Develop.* **21**, 37–47.

HARRIS, M. T. & BASARAN, O. A. 1993 Capillary electrohydrostatics of conducting drops hanging from a nozzle in an electric field. *J. Colloid Interface Sci.* **161**, 389–413.

HARRIS, M. T. & BASARAN, O. A. 1995 Equilibrium shapes and stability of nonconducting pendant drops surrounded by a conducting fluid in an electric field. *J. Colloid Interface Sci.* **170**, 308–319.

HARRIS, M. T. & BYERS, C. H. 1989 *An Advanced Technique for Interfacial Tension Measurement in Liquid-Liquid Systems*. ORNL/TM-10734.

HAYATI, I., BAILEY, A. I. & TADROS, TH. F. 1986 Mechanism of stable jet formation in electrohydrodynamic atomization. *Nature* **319**, 41–43.

INKPEN, S. L. & MELCHER, J. R. 1987 Dominant mechanisms for color differences in the mechanical and the electrostatic spraying of metallic paints. *Indust. Engng Chem. Res.* **26**, 1645–1653.

JOFFRE, G., PRUNET-FOCH, B., BERTHOMME, S. & CLOUPEAU, M. 1982 Deformation of liquid menisci under the action of an electric field. *J. Electrostatics* **13**, 151–165.

MELCHER, J. R. & TAYLOR, G. I. 1969 Electrohydrodynamics: A review of the role of interfacial shear stresses. *Ann. Rev. Fluid Mech.* **1**, 111–146.

MESTEL, A. J. 1994 Electrohydrodynamic stability of a slightly viscous jet. *J. Fluid Mech.* **274**, 93–113.

MICHAEL, D. H. 1981 Meniscus stability. *Ann. Rev. Fluid Mech.* **13**, 189–215.

MILLER, C. A. & SCRIVEN, L. E. 1970 Interfacial instability due to electrical forces in double layers. I. General considerations. *J. Colloid Interface Sci.* **33**, 360–370.

PEREGRINE, D. H., SHOLER, G. & SYMON, A. 1990 The bifurcation of liquid bridges. *J. Fluid Mech.* **212**, 25–39.

RAYLEIGH, LORD 1882 On the equilibrium of liquid conducting masses charged with electricity. *Phil. Mag.* **14**, 184–186.

REITZ, J. R. & MILFORD, F. J. 1967 *Foundations of Electromagnetic Theory*. Addison-Wesley.

SANKARAN, S. & SAVILLE, D. A. 1993 Experiments on the stability of a liquid bridge in an axial electric field. *Phys. Fluids* A **5**, 1081–1083.

SAVILLE, D. A. 1970 Electrohydrodynamic stability: fluid cylinders in longitudinal electric fields. *Phys. Fluids* **13**, 2987–2994.

SAVILLE, D. A. 1971 Electrohydrodynamic stability: effects of charge relaxation at the interface of a liquid jet. *J. Fluid Mech.* **48**, 815–827.

SCHULKES, R. M. S. M. 1994 The evolution and bifurcation of a pendant drop. *J. Fluid Mech.* **278**, 83–100.

SHI, X. D., BRENNER, M. P. & NAGEL, S. R. 1994 A cascade of structure in a drop falling from a faucet. *Science* **265**, 219–222.

TAKAMATSU, T., HASHIMOTO, Y., YAMAGUCHI, M. & KATAYAMA, T. 1981 Theoretical and experimental studies of charged drop formation in a uniform electric field. *J. Chem. Engng Japan* **14**, 178–182.

TAKAMATSU, T., YAMAGUCHI, M. & KATAYAMA, T. 1983 Formation of single charged drops in a non-uniform electric field. *J. Chem. Engng Japan* **16**, 267–272.

TAYLOR, G. I. 1964 Disintegration of water drops in an electric field. *Proc. R. Soc. Lond.* A **280**, 383–397.

TAYLOR, G. I. 1969 Electrically driven jets. *Proc. R. Soc. Lond.* A **313**, 453–475.

VU, N. & CARLESON, T. E. 1986 Electric field effects on drop size and terminal velocity in liquid-liquid systems. *AIChE J.* **32**, 1739–1742.

WHAM, R. M. & BYERS, C. H. 1987 Mass transport from single droplets in imposed electric fields. *Sep. Sci. Technol.* **22**, 447–453.

ZELENY, J. 1915 On the conditions of instability of electrified drops, with applications to the electrical discharge from liquid points. *Proc. Camb. Phil. Soc.* **18**, 71–83.

ZELENY, J. 1917 Instability of electrified liquid surfaces. *Phys. Rev.* **10**, 1–6.

ZHANG, X., HARRIS, M. T. & BASARAN, O. A. 1994 Measurement of dynamic surface tension by a growing drop technique. *J. Colloid Interface Sci.* **168**, 47–60.

ZHANG, X. & BASARAN, O. A. 1995 An experimental study of dynamics of drop formation. *Phys. Fluids* **7**, 1184–1203.

ZHANG, X., BASARAN, O. A. & WHAM, R. M. 1995 Theoretical prediction of electric field-enhanced coalescence of spherical drops. *AIChE J.* **41**, 1629–1639.

ZHANG, X., PADGETT, R. S. & BASARAN, O. A. 1996 Nonlinear deformation and breakup of stretching liquid bridges. *J. Fluid Mech.* in press.